Journal of Chemical Health Risks

www.jchr.org

JCHR (2025) 15(5), 2061-2073 | ISSN:2251-6727

"Evaluating the Efficacy of *Moringa oleifera*-Mediated Zinc Oxide Nanoparticles for Antifouling and Wound Healing Applications"

Singhai, Akansha[1]; Narkhede, Snehal[1]; Phillips, Enosh[1,2]; Dadsena, Ashish[1]; Sahu, Reecha[3]; Kush Kumar Nayak[4]; Laxmi Kant Pandey[2] ; Sur, Arunima[1*]

[1]Amity Institute of Biotechnology, Amity University Chhattisgarh, India

[3]Biomedical Engineering and Bioinformatics, University Teaching Department, Chhattisgarh Swami Vivekanand Technical University, India

Formally, affiliated to Amity Institute of Biotechnology, Amity University Chhattisgarh

[2]St. Aloysius College, Jabalpur

[4]School of Studies in Biotechnology, Shaheed Mahendra Karma University, Bastar, India

Formally, affiliated to Amity Institute of Biotechnology, Amity University Chhattisgarh

[*]Corresponding Author: Arunima Sur

(Received: 16 August 2025 Revised: 20 September 2025 Accepted: 01 October 2025)

KEYWORDS

Zinc oxide nanoparticles, Antibacterial activity, Antifouling, Wound healing, Moringa oleifera.

ABSTRACT:

The present study explores the green synthesis of zinc oxide nanoparticles (ZnO NPs) using Moringa oleifera leaf extract and evaluates their efficacy in antifouling and wound healing applications. The phytochemicals present in the extract acted as reducing and stabilizing agents, producing crystalline ZnO NPs confirmed by X-ray diffraction (XRD), which exhibited characteristic peaks corresponding to the hexagonal wurtzite structure (JCPDS card no. 36-1451). Field Emission Scanning Electron Microscopy (FE-SEM) revealed heterogeneous particle morphologies, including flower-like clusters with high surface area, while Fourier Transform Infrared Spectroscopy (FTIR) confirmed ZnO bond formation and the presence of bioorganic capping groups. The nanoparticles exhibited a zeta potential of –31.7 mV, indicating good colloidal stability. Antibacterial activity, assessed by well diffusion against Staphylococcus aureus and Pseudomonas aeruginosa, showed inhibition zones ranging from 12–16 mm (Moringa extract), compared to 20 mm for tetracycline (30 µg). Minimum inhibitory concentration (MIC) assays further confirmed dose-dependent inhibition at concentrations between 100–500 µg/mL. Antifouling activity evaluated via the crystal violet assay demonstrated marked inhibition of biofilm formation compared to untreated controls. Mechanistic studies suggested that ZnO NPs induce bacterial growth suppression primarily through reactive oxygen species (ROS) generation, disruption of cell membranes, and interference with protein and DNA integrity. Protein profiling by SDS-PAGE and DNA gel electrophoresis further validated the inhibitory impact on bacterial cellular machinery. Collectively, these findings demonstrate that M. oleifera-mediated ZnO NPs exhibit significant antibacterial, antibiofilm, and biomolecular interference activities, positioning them as sustainable and multifunctional candidates for next-generation wound healing and antifouling therapies.

Journal of Chemical Health Risks

www.jchr.org

JCHR (2025) 15(5), 2061-2073 | ISSN:2251-6727

Introduction

The effective management of wounds remains a pressing challenge in modern healthcare, particularly in cases complicated by microbial infections, biofilm formation, and delayed tissue regeneration. Chronic wounds and persistent ulcers not only reduce the quality of life of patients but also impose significant financial burdens on healthcare systems worldwide (Ali et al., 2025). Conventional therapies such as gauze dressings, topical ointments, and systemic antibiotics often fall short in providing long-term solutions, as they primarily offer symptomatic relief and are limited by poor antimicrobial protection, inadequate moisture retention, and reduced capacity to stimulate tissue repair. Moreover, the emergence of antibiotic-resistant pathogens and biofilm-associated infections further complicates wound healing, underscoring the need for advanced therapeutic strategies that can simultaneously address infection control and tissue regeneration (Wafy et al., 2025).

Nanotechnology has emerged as a promising platform for designing multifunctional biomaterials capable of overcoming these limitations. Zinc oxide nanoparticles (ZnO NPs), in particular, have attracted significant interest due to their broad-spectrum antimicrobial properties, ability to disrupt biofilms, and inherent biocompatibility. Beyond their antifouling activity, ZnO NPs have been reported to stimulate cell proliferation, collagen synthesis, and angiogenesis, all of which are critical processes in wound closure. Despite these benefits, conventional methods for synthesizing ZnO NPs often rely on toxic precursors and energy-intensive processes, raising concerns about safety and environmental sustainability (Al-Timimi et al., 2025).

Green synthesis strategies have therefore gained prominence as eco-friendly alternatives, with plant extracts serving as reducing, stabilizing, and capping agents. *Moringa oleifera*, a medicinal plant rich in bioactive phytochemicals such as flavonoids, phenolics, and terpenoids, provides a sustainable route for nanoparticle synthesis. These phytochemicals not only facilitate nanoparticle formation but also impart additional antimicrobial, antioxidant, and anti-inflammatory properties, thereby enhancing the biomedical utility of ZnO NPs. Furthermore, integrating *Moringa*-mediated ZnO NPs into biopolymer-based delivery systems, such as nanogels, can improve nanoparticle stability, regulate release kinetics, and create a moist wound environment conducive to healing (Mondal et al., 2025a).

In this context, the present study aims to evaluate the efficacy of *Moringa oleifera*-mediated ZnO nanoparticles for dual applications in antifouling and wound healing. By combining the advantages of green nanotechnology and natural biomaterials, this work seeks to establish a sustainable and clinically relevant platform capable of addressing microbial resistance, preventing biofilm formation, and accelerating tissue repair (Nandhini et al., 2025).

1. Emerging Role of Nanomaterials in Antifouling and Wound Healing

The management of wounds and the prevention of microbial colonization are central challenges in clinical practice. Wound healing is a dynamic, multi-stage process involving hemostasis, inflammation, proliferation, and

Journal of Chemical Health Risks
www.jchr.org
JCHR (2025) 15(5), 2061-2073 | ISSN:2251-6727

remodeling, all of which must progress in a coordinated manner to restore skin integrity. However, this process is often hindered by microbial contamination, biofilm formation, and drug-resistant pathogens, leading to delayed healing and chronic wounds. In parallel, antifouling strategies have gained importance in biomedical sciences, as the prevention of microbial adhesion and biofilm development on biological surfaces is crucial to reducing infection risk and enhancing therapeutic outcomes (Sellappan & Manoharan, 2024).

Nanomaterials have emerged as transformative tools in this domain due to their unique physicochemical properties, including high surface-to-volume ratio, tunable size, and multifunctionality. These attributes enable them to interact at the molecular and cellular level, thereby offering advantages over conventional antimicrobial and wound care agents. Various nanostructures such as metallic nanoparticles, polymeric nanogels, nanofibers, and nanocomposites have been developed to address both antifouling and wound healing challenges. Among them, metal oxide nanoparticles, particularly zinc oxide (ZnO), silver (Ag), and titanium dioxide (TiO_2), are noteworthy for their broad-spectrum antimicrobial activity, biofilm disruption potential, and ability to stimulate tissue regeneration (Liu et al., 2024).

Beyond their antimicrobial roles, nanomaterials can accelerate wound repair by promoting keratinocyte proliferation, collagen deposition, angiogenesis, and controlled drug release at the wound site. Additionally, their incorporation into advanced biomaterials such as hydrogels, nanogels, and scaffolds provides sustained therapeutic delivery, moisture retention, and mechanical stability, all of which are essential for optimal wound management. Importantly, green synthesis approaches using plant extracts, natural polymers, and other eco-friendly agents are being increasingly explored to overcome the toxicity and environmental concerns associated with conventional nanoparticle fabrication (Kirubakaran et al., 2024).

Given their dual ability to inhibit microbial fouling and accelerate tissue repair, nanomaterials represent a promising frontier in biomedical research. The convergence of nanotechnology with antifouling and wound healing strategies holds the potential to revolutionize next-generation wound care systems that are sustainable, multifunctional, and clinically effective (Mondal et al., 2025b).

2. Experimental Procedure Materials

Zinc chloride, Hi-LR ($ZnCl_2$) were purchased from Himedia and Sodium Hydroxide Pellets 98% (NaOH) were purchased from Loba Chemie Pvt. Ltd. were used further without any purification. Milli Q water was used throughout the experiments. Leaf samples of *M. oleifera* were collected from nearby areas of Nagpur region, Maharashtra, India and were brought to laboratory.

2.1. Synthesis of Zinc Oxide nanoparticles *via Moringa oleifera* leaves extract

Fresh leaves of *Moringa oleifera* were initially washed with tap water followed by three successive rinses using 25 mL portions of deionized water to eliminate dust and surface impurities. The cleaned leaves were then air-dried at room temperature, after which 10 g of

Journal of Chemical Health Risks
www.jchr.org
JCHR (2025) 15(5), 2061-2073 | ISSN:2251-6727

the dried material was finely chopped and transferred into a glass beaker containing 100 mL of deionized water. The mixture was heated at 50 °C for 30 minutes, resulting in a dark-colored extract. Once cooled to ambient temperature, the solution was filtered through Whatman No. 1 filter paper and preserved at 4 °C for subsequent synthesis.

2.2. Synthesis of Zinc Oxide Nanoparticles

To prepare ZnO nanoparticles, 40 mL of a 0.1 M zinc chloride ($ZnCl_2$) solution was combined with 10 mL of the prepared *M. oleifera* leaf extract (10 wt%). The reaction mixture was continuously stirred at 60 °C for two hours. A gradual color change from violet to yellow indicated the successful formation of ZnO nanoparticles. The nanoparticles were then separated by centrifugation at 7500 rpm for 15 minutes, thoroughly washed with deionized water to remove residual impurities, and dried at 80 °C for four hours. Finally, the dried product was calcined at 400 °C for two hours to obtain crystalline ZnO nanoparticles, which were subsequently ground into a fine powder for further characterization.

2.3. Field Emission Scanning Electron Microscopy (FESEM)

Field Emission Scanning Electron Microscopy (FESEM) was utilized to examine the surface morphology and structural features of the nanogel. This high-resolution imaging technique allowed detailed visualization of surface textures, pore distribution, and overall morphology, providing essential insights into the physical characteristics and potential applications of the nanogel (Al-Busaidi et al., 2025).

2.4. X-Ray Diffraction (XRD)

X-Ray Diffraction (XRD) analysis was performed to investigate the crystalline structure of the nanogel. This method provided information on the molecular arrangement, phase composition, degree of crystallinity, and presence of amorphous regions. Understanding the crystalline properties is crucial for predicting the material's stability and mechanical behavior (Sahai et al., 2024).

2.5. Fourier Transform Infrared Spectroscopy (FTIR)

Fourier Transform Infrared Spectroscopy (FTIR) was carried out to identify the functional groups and confirm the chemical composition of the nanogel. This technique detected specific chemical bonds and verified the incorporation of keratin and polyvinyl alcohol (PVA) within the nanogel matrix. The FTIR spectra exhibited characteristic absorption bands corresponding to various functional groups, confirming successful chemical modifications (Subbaiyan et al., 2024).

2.6. Zeta Potential Analysis

Zeta potential analysis was conducted to evaluate the surface charge of the nanogel. This technique provides insight into the stability and dispersion behavior of colloidal systems. Measurements were taken using a zeta potential analyzer, which applies an electric field to the suspended particles and tracks their movement. The direction and magnitude of particle migration reveal information about surface charge, helping to understand electrostatic interactions and predict the nanogel's stability

Journal of Chemical Health Risks
www.jchr.org
JCHR (2025) 15(5), 2061-2073 | ISSN:2251-6727

under different conditions(Nasir & Zahra, 2024).

2.7. Antibacterial Activity of Biosynthesized ZnO Nanoparticles

The antibacterial potential of the biosynthesized ZnO nanoparticles was assessed using the well diffusion method. Staphylococcus aureus and Pseudomonas aeruginosa were evenly spread on Mueller-Hinton agar plates. After allowing the plates to dry for 10 minutes, wells were created using a sterile micropipette tip, and 50 µL of ZnO nanoparticle solutions at different concentrations were added. The plates were then incubated at 37°C for 24 hours, and the diameters of the inhibition zones were measured in millimeters to evaluate antibacterial efficacy(Mazarei et al., 2025).

2.8. Mechanism of Bacterial Inhibition.

The antibacterial potential of *Moringa oleifera*-derived zinc oxide nanoparticles (ZnO NPs) was investigated against *Escherichia coli* following 24 hours of incubation. Cultures treated with ZnO NPs and tetracycline (Tet30) showed reduced turbidity and the presence of compact bacterial pellets after centrifugation, signifying inhibited growth and cell damage (Al-Fori et al., 2014). The inhibitory action is mainly linked to the ability of ZnO NPs to trigger the production of reactive oxygen species (ROS), which compromise membrane integrity, disturb permeability, and interfere with essential biomolecules such as proteins and DNA. When combined with tetracycline, the nanoparticles demonstrated enhanced activity through simultaneous disruption of membrane function and inhibition of protein synthesis. Collectively, these findings highlight that *Moringa oleifera*-mediated ZnO NPs possess strong antibacterial properties, reinforcing their potential applications in antifouling strategies and wound healing formulations (Ayyaru et al., 2020).

2.9. Protein extraction by TCA/acetone precipitation method and gel electrophoresis

The isolated bacterium was grown in NB with shaking incubator (120 rpm) at 37 °C for 48 h (Chaudhuri et al., 2016). After incubation, the cultures were centrifuged at 8000 rpm at 4 °C for 15 min and the CFSs were collected (Gowda et al., 2021). Then, the CFS was subjected to equal volume of acetone for protein precipitation by following the standard protocol of (Koontz et al., 2014) and the precipitated protein samples were resuspended in 100 µL of 2X SDS buffer (Bukhari et al., 2021).

2.10. Antifouling Activity of ZnO NPs (Crystal Violet Assay)

Using the crystal violet tube method, Moringa oleifera-derived ZnO nanoparticles showed strong antifouling activity(Mandalapu & Yanamala, 2025). Compared to controls with dense biofilm staining, ZnO NP-treated tubes exhibited markedly reduced violet coloration, indicating effective inhibition of bacterial adhesion and biofilm formation (Cheng et al., 2019).

3. Result

3.1. Characterized ZnO (NPs)

Journal of Chemical Health Risks

www.jchr.org

JCHR (2025) 15(5), 2061-2073 | ISSN:2251-6727

Field Emission Scanning Electron Microscopy (FE-SEM):

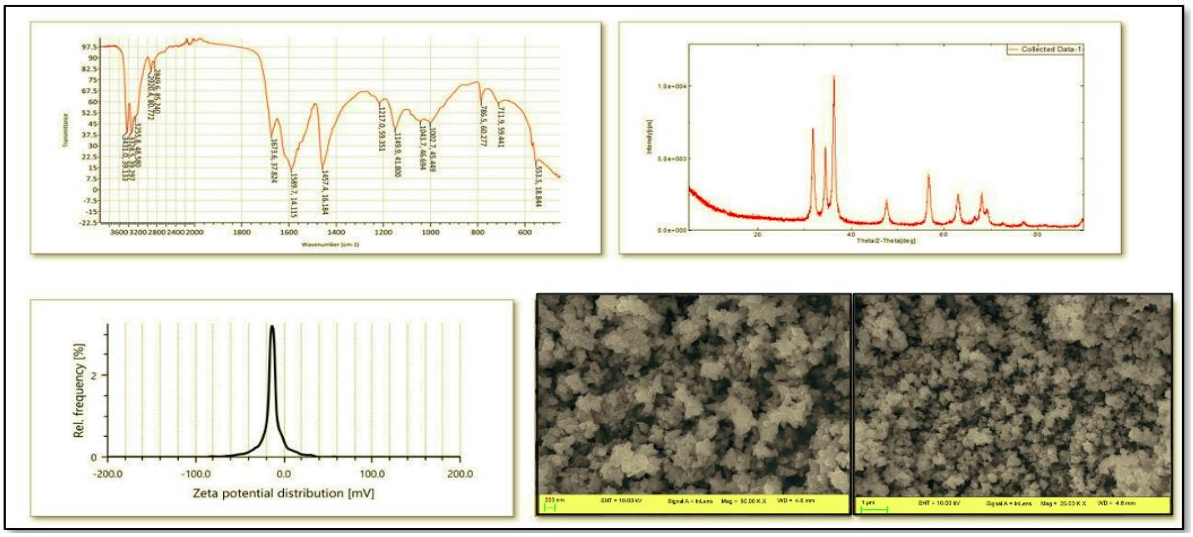

Fig 1: FTIR, XRD, Zeta Potential, and FE-SEM Analyses of Synthesized ZnO Nanoparticles.

FE-SEM imaging confirmed the formation of ZnO nanoparticles, revealing both individual particles and clustered, flower-like architectures. These complex morphologies suggest that the phytochemicals present in the plant extract effectively mediated both reduction and stabilization during synthesis. The flower-shaped assemblies highlight the ability of green synthesis routes to yield structurally diverse nanomaterials with enhanced surface area, making them suitable for functional applications. Comparable morphological patterns have also been observed in other studies on plant-assisted ZnO nanoparticle synthesis, reinforcing the reliability of this method.

3.2. X-Ray Diffraction (XRD):

XRD analysis validated the crystalline nature of the biosynthesized ZnO nanoparticles. The diffraction peaks corresponded to the characteristic hexagonal wurtzite structure, with a prominent reflection around 36° (2θ) indexed to the (101) plane. Additional peaks near 31°, 34°, 47°, 56°, and 63° (2θ) aligned with standard reference data (JCPDS card no. 36-1451), confirming phase purity and high crystallinity. Such crystallinity is directly linked to improved photocatalytic performance and thermal stability, as reported in previous ZnO studies.

3.3. Fourier Transform Infrared Spectroscopy (FTIR):

FTIR spectra provided insight into the surface chemistry of the nanoparticles. The characteristic absorption bands at lower wavenumbers confirmed Zn–O bond formation, while peaks at higher wavenumbers indicated the presence of organic groups originating from the plant extract. These biomolecules serve as natural capping and stabilizing agents, contributing to controlled particle size distribution and improved dispersion. This dual role of phytochemicals in

Journal of Chemical Health Risks
www.jchr.org
JCHR (2025) 15(5), 2061-2073 | ISSN:2251-6727

nanoparticle synthesis has been widely recognized in other plant-mediated approaches.

3.4. Zeta Potential Analysis:

The zeta potential of the synthesized ZnO nanoparticles was measured to assess their colloidal stability. A value of –31.7 mV was obtained, indicating good stability due to electrostatic repulsion between negatively charged particles. This stability minimizes aggregation and ensures uniform dispersion, which is crucial for applications requiring prolonged suspension such as environmental remediation and biomedical systems. The negative charge also facilitates strong interactions with microbial cells and pollutants, enhancing antimicrobial and photocatalytic activity.

3.5. Antibacterial Activity of ZnO nanoparticles

The antibacterial potential of the test samples was assessed against *Pseudomonas aeruginosa* using the zone of inhibition assay. The control group (D) showed no inhibitory effect, whereas the standard antibiotic tetracycline (30 µg) exhibited a prominent inhibition zone of 20 mm, validating the assay. Among the extracts, green tea (G) demonstrated comparatively higher antibacterial activity, with inhibition zones ranging from 14 to 18 mm. In contrast, Moringa (M) exhibited relatively lower activity, producing inhibition zones between 12 and 16 mm. Overall, green tea extract showed stronger inhibitory potential against *P. aeruginosa* than Moringa, although both were less effective than the standard tetracycline.

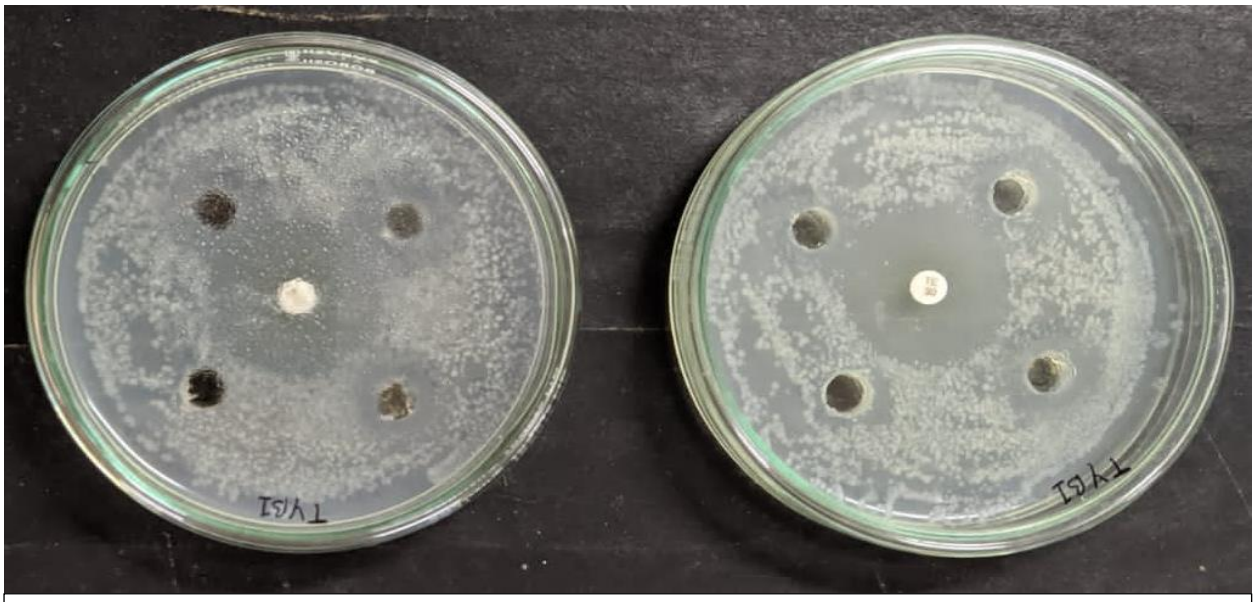

Fig 2 : Antibacterial Activity Against *Pseudomonas aeruginosa*

Journal of Chemical Health Risks

www.jchr.org

JCHR (2025) 15(5), 2061-2073 | ISSN:2251-6727

3.6. Minimum Inhibitory Concentration of Zinc Oxide Nanoparticles:

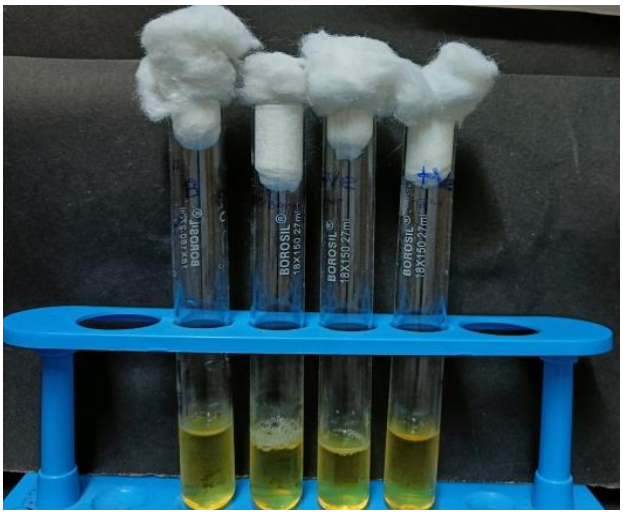

Fig 3 A- Minimum Inhibitory Concentration of Zinc Oxide Nanoparticles-24 hr incubated

Fig 3 B- Bacterial pellet after addition of ZnONPs and Tet30

MIC was performed to check the minimum inhibitory concentration of the synthesized nanoparticles. Different concentrations of nanoparticles such as 50, 100, 200, 300, 400 and 500 µg/ml were added in different test tubes containing 5 ml of Nutrient Broth and then inoculated with bacterial culture along with positive and negative control. Tubes were incubated at 37°C for 24-48 hrs in rotary shaker incubator at 120 rpm and were observed for the growth.

The synthesized zinc oxide nanoparticles were checked for antibacterial activity and MIC. Antibacterial activity was performed by well diffusion method. Nutrient agar plates were used bacterial lawn was prepared on it and well were prepared. To the wells different concentrations of ZnO NPs were added as 25µl, 50µl and 100µl with negative (DMSO) and positive (Tetracycline 30 mcg) control. The plates were incubated at 37°C for 24hrs and zone of inhibition were recorded.

3.7. Protein estimation

BSA (1%) was prepared separately, according to the required volume. The protein content present in the CFSs of *Enterobacter and pseudomonas* was measured by following the Universal method of Lowry et al. [35]. The standard BSA (2 mg mL−1 in distilled water) samples were prepared in 0.1 N NaOH to get the concentrations of 40, 80, 120, 160 and 200 µg mL−1 in glass tubes in duplicates, respectively. The test samples, CFSs of B were taken in 2 different concentrations (0.2 and and 0.4 mL), respectively. An equal volume of alkaline copper reagent was added to all tubes and the mixture was incubated for 15 min at room temperature. Folin's reagent (Sigma, USA) was added at a concentration of 50 µL mL−1 . The entire contents was mixed well and incubated for 30 min at room temperature. Optical density (OD) was measured at 690 nm. The protein concentration in the samples was estimated from the graph plotted for the standard BSA concentrations.

Journal of Chemical Health Risks
www.jchr.org
JCHR (2025) 15(5), 2061-2073 | ISSN:2251-6727

3.8. SDS-PAGE

The protein sample was used for molecular weight determination and the protein content was estimated by following Lowry's method using tyrosine as standard (Lowry *et al*., 1951). The 40 µl of each protein sample was taken and mixed in 20 µl of sample buffer, after incubation for 5 min at 100°C. SDS-PAGE was performed by following the protocol of (Laemmli et al., 1970). The glass plates and spacers were thoroughly cleaned, dried and assembled properly using bulldog clips. Agar-agar (melted in a boiling water bath) was applied around the edges of the spacers to hold them in a place and the chamber was sealed between the glass plates. A sufficient volume of separating mixture was prepared, mixed gently and the gel solution was poured in the chamber between the plates. Distilled water was layered on the top of the gel and left to set for 45 min. Once the separating gel was set, the water layer was removed from the top of the gel and washed with little stacking gel solution. After pouring stacking gel mixture (appendix), the comb was placed in the stacking gel. The cathode was connected at the top and direct current power was switched on briefly to check the electric current. The current was turned on initially for 30 min at 50V until the samples travelled through the stacking gel. Then it was run at 100V until the dye reached the bottom of the gel. After running, the gel slab was stained in Coomassie brilliant blue for 45 min, followed by de-staining in destainer till distinct bands were obtained. The protein profile obtained in the gel was documented .

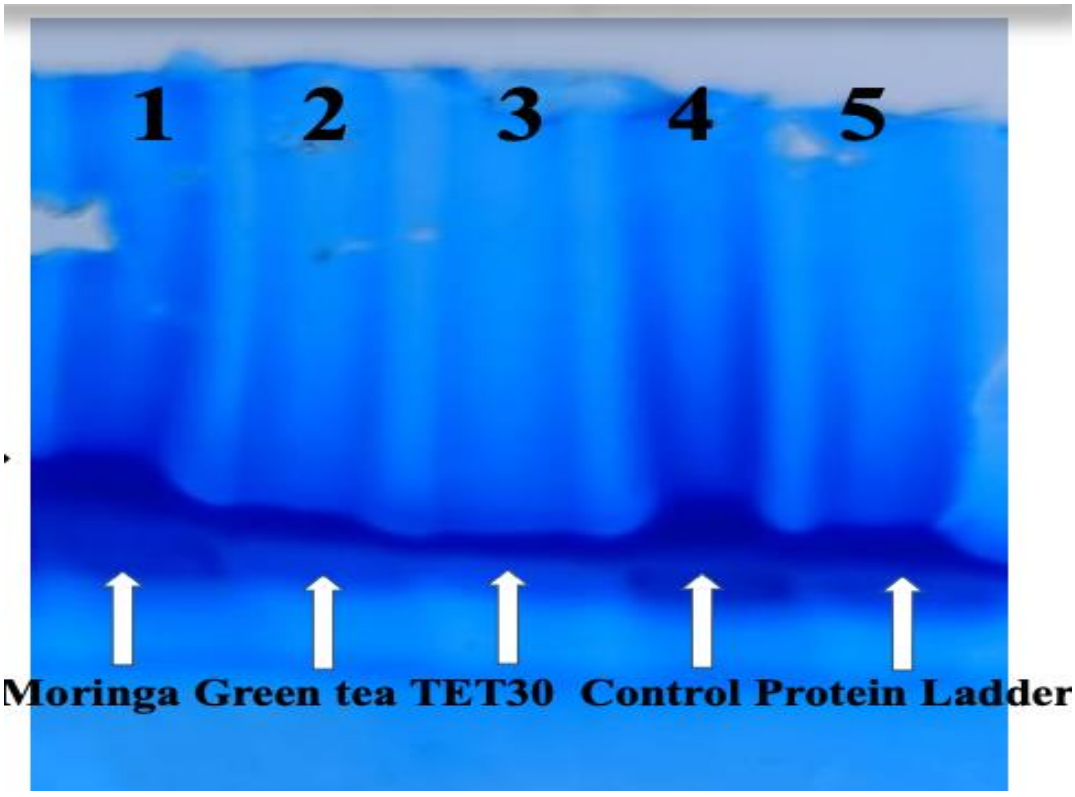

Fig 4 -SDS-PAGE Analysis of Protein Sample

Journal of Chemical Health Risks
www.jchr.org
JCHR (2025) 15(5), 2061-2073 | ISSN:2251-6727

3.9. DNA electrophoresis

Total genomic DNA was isolated from the bacterial pure cultures grown to the late exponential phase by means of a standard protocol (Ausubel et al., 2003) as follows: 1.5 ml of the overnight bacterial culture (grown in the LB medium) was transferred to a 1.5 ml Eppendorf tube and centrifuged at 13000 rpm for 1 min to pellet the cells. The supernatant was discarded. The cell pellet was suspended in 600 μl TE buffer and centrifuged at 13000 rpm and the supernatant discarded. The cell pellet was resuspended in 200 μl TE buffer, and the following were added: 5 μl lysozyme (20 mg/ml), 5 μl RNAnase (20 mg/ml), and 10 μl proteinase K (20 mg/ml) followed by overnight incubation at 37°C. In the next morning, the temperature was adjusted to 56°C for one hr and an equal volume of phenol/chloroform (1 : 1) was added and mixed well by inverting the tube until the phases were completely mixed. Spinning was done at 13000 rpm for 15 min at room temperature. The upper aqueous phase was carefully transferred to a new tube by using 1 ml pipette. This step was repeated twice to ensure all protein had been removed. An equal volume of chloroform and isoamyl (24 : 1) was added to the aqueous layer and centrifuged at 13000 rpm for 15 min. The aqueous layer was removed into a new tube. This step was also repeated to ensure all phenol is removed. An equal volume of isopropanol was added and stored overnight at −20°C. The samples were then defrosted and centrifuged at 4°C for 30 min to pellet the DNA. The pellet was washed in 70% ethanol and centrifuged at 13000 rpm for 5 min, and then, the ethanol was carefully pipetted out. The pellet was air dried on the bench for 20 min, and the isolated genomic DNA was viewed on a 1% agarose gel.

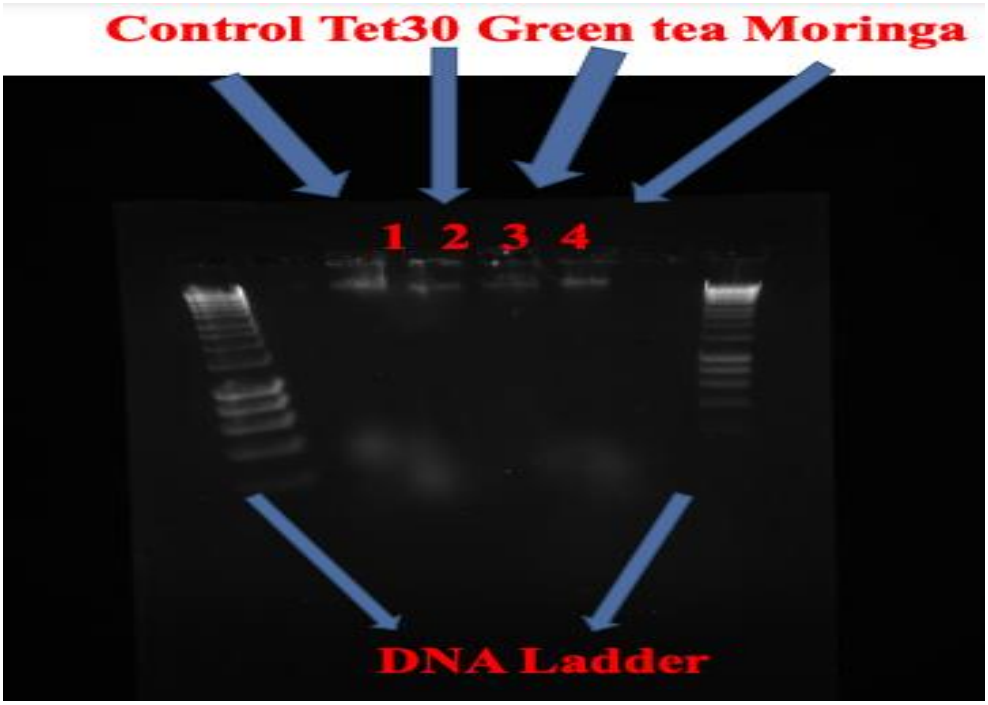

Fig 5 - DNA estimation by Gel Electrophoresis

Journal of Chemical Health Risks

www.jchr.org

JCHR (2025) 15(5), 2061-2073 | ISSN:2251-6727

3.10. Antifouling Activity of ZnO NPs (Crystal Violet Assay)

Antifouling activity was performed by using 24-48hrs fresh grown culture in test tube containing bacterial for biofilm production incubated at 37°C. To other test tubes nanoparticles were added in the bacterial broth as well as positive control and negative control was added to it. The test tubes were further incubated at 37°C to observe for antifouling activity. The test tubes were decanted to observe for biofilm production. To these test tubes crystal violet stain was added and kept for 2-3 minutes for contact time and tubes were washed with distilled water and air dried to observe for antifouling activity.

4. Conclusion:

The study successfully demonstrated the eco-friendly synthesis of ZnO nanoparticles using *Moringa oleifera* leaf extract, yielding crystalline, stable, and bioactive nanostructures. Characterization confirmed the dual role of phytochemicals as reducing and capping agents, which not only facilitated particle formation but also enhanced antimicrobial activity. The synthesized ZnO NPs showed effective antibacterial activity against Gram-positive and Gram-negative pathogens, inhibited biofilm formation, and induced protein and DNA damage in bacterial cells. These combined properties underscore their potential as multifunctional nanomaterials for advanced wound care. By addressing infection, biofilm formation, and delayed tissue repair simultaneously, *Moringa*-derived ZnO NPs provide a sustainable and clinically relevant alternative to conventional therapies.

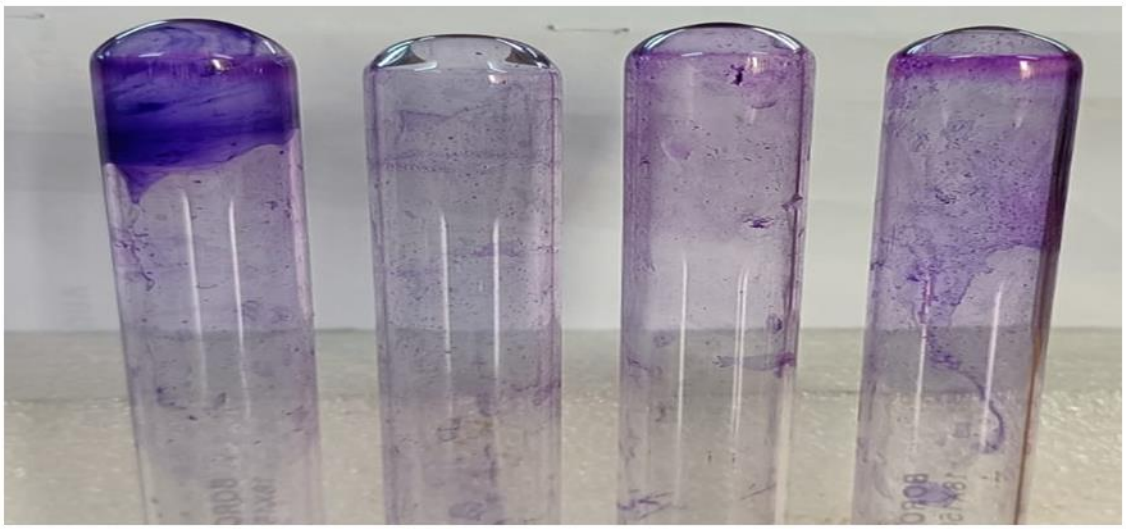

Fig 6: Test Tube Assay Using Crystal Violet for Biofilm Inhibition

Journal of Chemical Health Risks

www.jchr.org

JCHR (2025) 15(5), 2061-2073 | ISSN:2251-6727

5. Future perspective :

Moringa oleifera-mediated ZnO nanoparticles show strong promise as sustainable materials for next-generation biomedical use. Their proven antibacterial and antibiofilm activities suggest they can be effectively incorporated into nanogels, hydrogels, and wound dressings to accelerate healing while preventing infections. Future research should focus on in vivo validation to confirm their role in promoting angiogenesis and tissue regeneration. Beyond wound care, their antifouling ability makes them suitable for coating medical devices and implants. With scalable green synthesis, these nanoparticles offer a safe, eco-friendly, and commercially viable platform to improve healthcare outcomes.

6. Conflicts of interest

The authors have no conflict of interest to declare in this study.

References

1. Al-Busaidi, A., Al-Mamari, R., Kyaw, H. H., Myint, M. T. Z., Al-Abri, M., & Dobretsov, S. (2025). Antifouling properties of copper oxide microparticles and zinc oxide nanoparticles in greenhouse cooling systems. *Frontiers in Nanotechnology*, *7*, 1545224.
2. Al-Fori, M., Dobretsov, S., Myint, M. T. Z., & Dutta, J. (2014). Antifouling properties of zinc oxide nanorod coatings. *Biofouling*, *30*(7), 871–882.
3. Ali, S., Mirza, R., Shah, K. U., Javed, A., & Dilawar, N. (2025). Harnessing green synthesized zinc oxide nanoparticles for dual action in wound management: Antibiotic delivery and healing Promotion. *Microbial Pathogenesis*, 107314.
4. Al-Timimi, Z., Haddawi, S. F., & Nukhailawi, S. A. H. (2025). Comparative histological assessment of zinc oxide nanoparticles and low-power laser treatment at 810nm wavelength on the recovery of second-degree burn wounds in rat models. *The International Journal of Lower Extremity Wounds*, 15347346241313008.
5. Ayyaru, S., Dinh, T. T. L., & Ahn, Y.-H. (2020). Enhanced antifouling performance of PVDF ultrafiltration membrane by blending zinc oxide with support of graphene oxide nanoparticle. *Chemosphere*, *241*, 125068.
6. Bukhari, A., Ijaz, I., Gilani, E., Nazir, A., Zain, H., Saeed, R., Alarfaji, S. S., Hussain, S., Aftab, R., & Naseer, Y. (2021). Green synthesis of metal and metal oxide nanoparticles using different plants' parts for antimicrobial activity and anticancer activity: a review article. *Coatings*, *11*(11), 1374.
7. Chaudhuri, B., Alam, N., Sarkar, M., Chowdhury, T., & Chattopadhyay, B. (2016). Phylogenetic characterization of BKH3 bacterium isolated from a hot spring consortium of Bakreshwar (India) and its application. *Advances in Microbiology*, *6*(6), 453–461.
8. Cheng, H., Guan, Q., Villalobos, L. F., Peinemann, K.-V., Pain, A., & Hong, P.-Y. (2019). Understanding the antifouling mechanisms related to copper oxide and zinc oxide nanoparticles in anaerobic membrane bioreactors. *Environmental Science: Nano*, *6*(11), 3467–3479.
9. Gowda, A. S. P., Schaefer, A. D., & Schuck, T. K. (2021). Effect of excipients on recombinant interleukin-2 stability in aqueous buffers. *American Journal of Analytical Chemistry*, *12*(10), 347–372.
10. Kirubakaran, D., Selvam, K., Subramanian Shivakumar, M., Rajkumar, M., Kannan, S., & Navina, B. (2024). Bio-fabrication of Zinc oxide nanoparticles using Strobilanthes cordifolia: Characterization and evaluation of antioxidant, anti-cholinergic, anti-

Journal of Chemical Health Risks

www.jchr.org

JCHR (2025) 15(5), 2061-2073 | ISSN:2251-6727

inflammatory and wound healing activities. *ChemistrySelect*, *9*(6), e202302792.

11. Liu, Y., Ma, Q., Tang, L., Shen, Y., Zhao, H., Liu, X., Lin, D., & Zhou, G. (2024). A multifunctional hydrogel with mild photothermal antibacterial and antioxidant properties based on quercetin and dopamine-coated zinc oxide nanoparticles for healing bacteria-infected wound. *Chemical Engineering Journal*, *497*, 154518.
12. Mandalapu, V. R., & Yanamala, V. (2025). Comparative Study of Quantitative Estimation of Effect of An Organophosphate (Malathion) on TCA Precipitated Proteins in different Tissue of Two Fresh Water Fishes Channa punctatus and Labeo rohita. *INNOVATIVE TECHNIQUES IN ANIMAL BIOTECHNOLOGY AND IMMUNOLOGY FOR DISEASE PREVENTION & MANAGEMENT*, 56.
13. Mazarei, S., Safaie, M., Homaei, A., & Ghasemi, Z. (2025). Progress in tailor-made of anti-fouling coating strategies for marine fish farming cages based on green synthesis of zinc oxide nanoparticles from Avicennia marina leaves. *Progress in Organic Coatings*, *208*, 109465.
14. Mondal, M. I. H., Islam, M. M., & Ahmed, F. (2025a). Enhanced wound healing with biogenic zinc oxide nanoparticle-incorporated carboxymethyl cellulose/polyvinylpyrrolidone nanocomposite hydrogels. *Biomaterials Science*, *13*(1), 193–209.
15. Mondal, M. I. H., Islam, M. M., & Ahmed, F. (2025b). Enhanced wound healing with biogenic zinc oxide nanoparticle-incorporated carboxymethyl cellulose/polyvinylpyrrolidone nanocomposite hydrogels. *Biomaterials Science*, *13*(1), 193–209.
16. Nandhini, J., Karthikeyan, E., Sheela, M., Bellarmin, M., Kannan, B. G., Pavithra, A., Sri, D. S., Prakash, S. S., & Kumar, S. R. (2025). Optimization of microwave-assisted green synthesis of zinc oxide nanoparticles using Ocimum americanum and Euphorbia hirta extracts: In vitro evaluation of antioxidant, anti-inflammatory, antibacterial, cytotoxicity, and wound healing properties. *Intelligent Pharmacy*, *3*(1), 90–109.
17. Nasir, H., & Zahra, S. K. (2024). A Review Of Sustainable Methods For Synthesizing Zinc Oxide Nanoparticles And Their Applications. *Science Heritage Journal (GWS)*, *8*(1), 27–37.
18. Sahai, R. S. N., Khan, M. W., Jadhav, A., & Sharma, M. (2024). Antimicrobial polymer composites with anti-biofouling features for floating solar power plant applications: Effect of zinc oxide nanoparticles. *Polymers from Renewable Resources*, *15*(1), 78–89.
19. Sellappan, L. K., & Manoharan, S. (2024). Fabrication of bioinspired keratin/sodium alginate based biopolymeric mat loaded with herbal drug and green synthesized zinc oxide nanoparticles as a dual drug antimicrobial wound dressing. *International Journal of Biological Macromolecules*, *259*, 129162.
20. Subbaiyan, R., Ganesan, A., Muthusamy, B., & Ramasubramanian, B. (2024). Self potent antimicrobial and antifouling properties of zinc nanoparticles derived from lichen symbionts. *Environmental Progress & Sustainable Energy*, *43*(2), e14307.
21. Wafy, M. N., Hassan, E. A., Saeed, S., Khattab, M. S., AbuBakr, H. O., & Abu-Seida, A. M. (2025). Therapeutic Efficacy of Zinc Oxide Nanoparticles Ointment in Promoting Wound Healing in Dogs: A Clinical Study. *Journal of Applied Veterinary Sciences*.